

## The Performance Enhancement with the Use of New Generation Core Materials for Claw-Pole Synchronous Generators

Selami BALCI

Karamanoglu Mehmetbey University, Faculty of Engineering, Department of Electrical and Electronics Engineering, Karaman/Türkiye. ORCID: 0000-0002-3922-4824

Corresponding Author: sbalci@kmu.edu.tr

Arrival Date: 23.06.2024

Acceptance Date: 25.12.2024

### Abstract

Synchronous generators (also known as alternators) used in conventional vehicles can also be used to charge batteries in power systems of hybrid electric vehicles. As the alternator type, a synchronous generator with a claw pole (CPSG) is generally preferred, which has similar features to quadrature-axis flux synchronous generators. The pole structures of CPSGs are mostly excitation winding, but they can be designed as permanent magnets in recent years. In this study, comparative electromagnetic modeling and simulation of a 0.55 kVA rated power and 4-pole permanent magnet CPSG according to the core material type was performed with ANSYS-Electronics software. The performance of the proposed new generation core materials as amorphous and JFE supercore is investigated in comparison with the conventional core material (SiFe alloy). Thus, it has been determined that the JFE supercore material is a much more suitable core material in the stator design of CPSGs in terms of improving the performance in terms of core losses and efficiency. Comparative simulation studies have reported that the highest efficiency of approximately 87% is achieved using new generation core materials such as amorphous and jfe supercore. In addition, it was emphasized that a more compact generator could be designed thanks to the new generation core materials with high electromagnetic characteristics and the power density of a much higher kVA/kg.

**Keywords:** Claw-Pole Synchronous Generator, New Generation Core Materials, Core Losses, Finite Element Analysis (FEA) Modelling.

### Pençe-Kutuplu Senkron Generatörlerde Yeni Nesil Çekirdek Malzemelerin Kullanımıyla Performans Artışı

#### Özet

Geleneksel taşıtlarda kullanılan senkron generatörler (alternatör olarak da bilinir) hibrit elektrikli taşıtların güç sistemlerindeki bataryaları şarj etmek için de kullanılabilir. Alternatör tipi olarak genellikle, kare-eksen akılı senkron generatörlere benzer özelliklere sahip pençe kutuplu senkron generatör (CPSG) tercih edilir. CPSG'lerin kutup yapıları çoğunlukla uyarma sargılıdır, ancak son yıllarda kalıcı mıknatıslı olarak da tasarlanabilmektedir. Bu çalışmada, 0,55 kVA anma gücüne sahip ve 4 kutuplu kalıcı mıknatıslı bir CPSG'nin çekirdek malzeme tipine göre karşılaştırmalı elektromanyetik modellemesi ve benzetimi ANSYS-Electronics yazılımı ile yapılmıştır. Önerilen yeni nesil çekirdek malzemelerinin performansı amorf ve JFE super çekirdek olarak geleneksel çekirdek malzemesi (SiFe alaşımı) ile karşılaştırmalı incelenmiştir. Böylece, JFE süperçekirdek malzemesinin, çekirdek kayıpları ve verimlilik açısından performansı iyileştirme açısından CPSG'lerin stator tasarımında çok daha uygun bir çekirdek malzemesi olduğu belirlenmiştir. Gerçekleştirilen karşılaştırmalı benzetim çalışmaları ile en yüksek verimin yaklaşık %87 olarak amorf ve jfe supercore gibi yeni nesil nüve materyalleri kullanılarak sağlandığı rapor edilmiştir. Ayrıca, yüksek elektromanyetik özelliklere sahip yeni nesil çekirdek malzemeleri ve çok daha yüksek kVA/kg güç yoğunluğu sayesinde daha kompakt bir generatör tasarlanabileceği vurgulanmıştır.

**Anahtar Kelimeler:** Pençe-Kutuplu Senkron Generatör, Yeni Nesil Çekirdek Malzemeleri, Çekirdek Kayıpları, Sonlu Elemanlar Analizi (SEA) Modellemesi

NOMENCLATURE			
		Greek Symbols	
$B_m$	Magnetic flux density (Tesla)		
$E_{ph}$	Induced phase voltage of stator windings (Volts)	$\psi_d$	Direct axis of stator phase fluxes
$f$	Frequency (Hertz)	$\psi_q$	Quadrature-axis of stator phase fluxes
$K_e$	Coefficients for the eddy-current losses	$\varphi$	Phase angle
$K_h$	Coefficients for the hysteresis losses	$\Phi$	Magnetic flux (Weber)
$K_{wl}$	Coefficient of stator windings	$\Phi_m$	Maximum flux (Weber)
$N_w$	Number of turns for stator winding	$\mu_r$	Relative permeability
$R_c$	Stator winding resistance	$n_r$	Rotor speed (rpm)
$X_d$	Direct-axis reactance	$\omega$	Angular synchronous speed (rad./sec.)
$X_q$	Quadrature-axis reactance	$\mathcal{R}$	Magnetic circuit reluctance
$T_{cog}$	Cogging torque of synchronous generators	$\theta$	Rotor position angle



[Bu makale Creative Commons Attribution-NonCommercial-ShareAlike 4.0 International \(CC BY-NC-SA 4.0\) License ile lisanslanmıştır.](https://creativecommons.org/licenses/by-nc-sa/4.0/)

## 1. INTRODUCTION

To obtain electrical energy, different types of generators with rated power values ranging from a few kW to MW levels with varying design concepts depending on the usage area have been developed. Historically, the squirrel-cage induction generator has often been used commercially. A second popular type is the wound rotor generator, and the third is the separately excited synchronous generator. In this context, replacing the rotor excitation winding with permanent type magnets in a synchronous machine does not require the use of additional electrical and mechanical devices such as field windings, brush-ring arrangement, and excitation generators. At the same time, it is highly advantageous that a simple rotor design with direct drive (without gearbox) allows higher efficiency to be achieved with lower temperature rise and power loss. Permanent magnet synchronous machines are designed with three different rotor topologies: surface-mounted permanent magnets, embedded permanent magnets, and claw-pole configuration [1]. CPSGs are frequently preferred as automobile, wind and hydroelectric generators in the past literature due to their simple structure, multipolar design and low manufacturing costs. Thus, the high number of poles makes CPSGs an important alternative in variable speed systems such as automobiles. Permanent magnets replace the excitation coil in the rotor and increase the overall efficiency of the synchronous machine [2].

Traditionally, the claw-pole synchronous generator (CPSG) has been used with 100–200 W DC-excited power to the rotor and has been used only with controlled diode rectified output in road vehicles since 1975 due to its low cost, easy manufacturing, and high reliability despite the DC-conducting rings and brushes to the excitation windings. However, the overall efficiency (with diode rectifier, DC excitation, stator core, rotor claw eddy current and mechanical losses) is moderate (about 70% at 2.5 kW at 14 V DC and 6000 rpm). While using copper (aluminum) coils to increase the winding fill factor of the stator slots and thus further reduce copper losses, research continues the use of soft magnetic composites in core structures to reduce losses in the rotor, especially in the stators. [3, 4]. CPSGs are widely used for automobile generators. In addition, with the increase in hybrid and electric components in automobiles in recent years, the electrical power requirements have increased. For this reason, studies on the design and performance improvements of claw pole alternators, especially in hybrid electric vehicles (HEVs), have become one of the most important issues in automobile technologies [5]. The popularity of this type of generator is mainly due to the compact structural features of the multipole rotor design (integrating in a low volume) and the heteropolar structure of its rotor, which provides a distinctive electricity generation capability. However, despite these advantages, the CPG has two major drawbacks: its low efficiency, mainly due to the structural claw feature at the poles and the leakage fluxes between the poles, the use of a brush-ring system to feed the magnetic field in the rotor in types with excitation windings [6, 7, 8].

According to the degree of hybridization, hybrid vehicles can be divided into three categories: micro hybrid, mild hybrid, and heavy hybrid [9]. The electric motor of micro-hybrid vehicles is connected to the internal combustion engine via a belt-pulley system. When the internal combustion engine is idling for a long time, the control system in the vehicle automatically stops the engine. When the car needs to be restarted, the electric motor as the starter will quickly pull the engine from the belt to idle speed to realize the restart of the internal combustion engine. In other normal driving conditions, this electric motor is driven by the internal combustion engine (ICE) to generate electricity that powers the electrical devices and batteries inside the vehicle. Thus, the CPSG operates both as a starter motor and as a generator to generate electricity, so it is also called a belt-driven

starter generator (BSG). It uses low carbon steel (Steel 1008) as a base [10]. Therefore, many automakers are working on the standardization of this type of technology for all ICEs, gasoline, or diesel, small or large. The purpose of the electric machine used in a starter-alternator system is to both start the internal combustion engine and charge the lead-acid battery [11].

The development of more electric vehicles has been an important trend worldwide, driven by increasing energy consumption, the gradual reduction of fossil fuels and environmental protection concerns [12]. So far, the all-electric vehicle has suffered from issues such as a limited driving range and more time consumption for battery charging compared to refueling. Therefore, for now, HEVs can be considered a better transition option [13].

Claw pole alternators are a type of winding field synchronous machine with salient pole structure that can generate electricity in the stator coils, where the rotor acts as an electromagnet. It has been widely used in automobiles for many years to power batteries through the three-phase rectifier circuit as shown in Figure 1 [14]. In addition, a study conducted for six-pulse rectifier (three-phase full bridge rectifier circuit) load cases CPSG modeled with ANSYS-Maxwell 3D software. Filter circuits have been proposed for terminal voltage and current harmonic distortion problems for power quality [15]. Thus, the use of low-pass type filters significantly reduces the terminal voltage and current harmonic distortion levels for a six-pulse rectifier load [16].

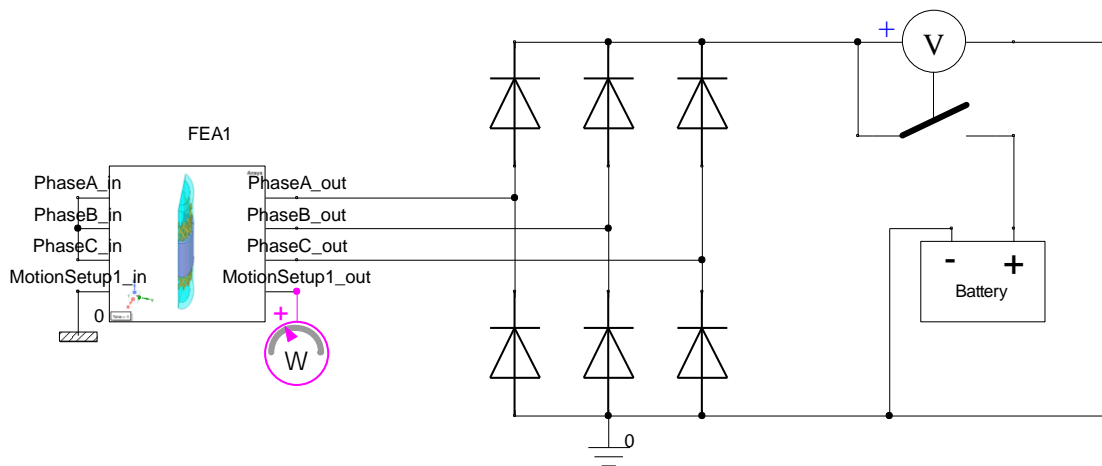


**Figure 1.** The basic topology of three-phase rectifier circuit connected to CPSGs

A permanent magnet claw pole machine can solve the mechanical problem in the brush-ring system and increase the power density (kVA/kg) and efficiency by reducing the dimensions of the permanent magnet (PM) excitation type machine [17]. On the other hand, the hybrid excitation method is very suitable for the power system of electric vehicles because of the difficulty of voltage adjustment in PM type excitation method and being easily affected by temperature changes [18, 19, 20]. In [21], the mechanical performance of a CPSG is calculated using 3D finite element analysis (FEA). Thus, the CPSG core volume was successfully reduced to 78% and the amount of permanent magnet used was also reduced by 4%. The air gap distance between the stator and rotor parts of claw pole alternators is greater than that of conventional salient pole generators. Thus, CPSGs have more air circulation and the more easier cooling [22]. On the other hand, new design approaches proposed in recent years are PMSG with permanent magnet excitation in the rotor and the phase windings only in the stator. The rotor of CPSG has four pieces of poles and is based on electromagnetic modeling and simulation studies using FEA software [13, 23].

In this study, a comparative modeling of a CPSG with 0.55 kVA rated power and 4 piece of PM poles, with a rated speed of 1500 rpm, was performed using FEA software. Comparative simulation studies were conducted for the case of using classical non-oriented M19 core (3% SiFe), JFE supercore material (10JNEX900) and amorphous core material (2605SA1) as stator core material. Thus, various suggestions have been made in terms of performance enhancement, reducing power losses, and improving efficiency, for the use of new generation core materials for CPSGs.

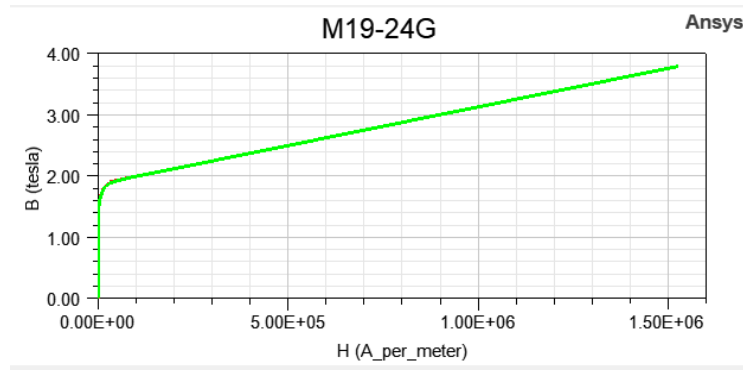
## 2. MATERIALS and METHODS

In recent years, soft magnetic composite materials have gained popularity due to their many unique properties such as high magnetic isotropy [24], much lower core losses, great mechanical design flexibility in magnetic circuit elements such as inductors, transformers and electric motors/generators, and great potential for mass production at very low cost. Research and development studies on technological development and their application in electromagnetic devices have become very popular [25].

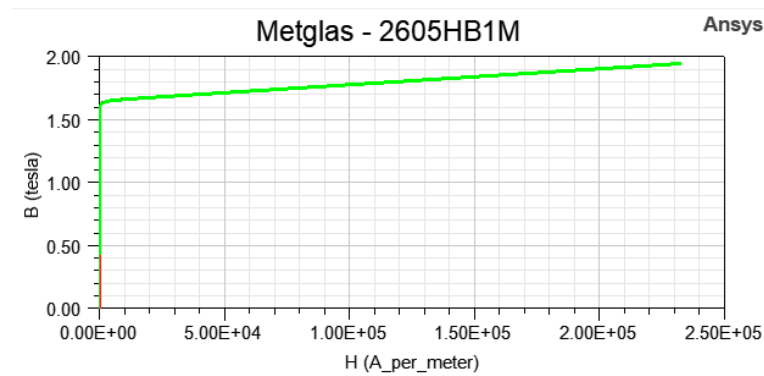
When designing electric motors or generators with new generation core materials, the accuracy of simulation studies is very important before prototype production in determining the real energy savings that can be expected from a new technology that is improved electrically and mechanically. In claw-pole generator design, modeling and simulation studies, it becomes very difficult to examine the control laws such as electromagnetic theory related to the realistic design of electrical machines, the temperature increases of the generator and the efficiency of the obtained electrical energy with classical methods [26]. In this section, a brief technical comparison of the classical core material and the new generation core materials is made. Also, the electromagnetic modeling approach and the steps of simulation studies are explained with the FEA software.

### 2.1. Technical Comparison of the Core Materials

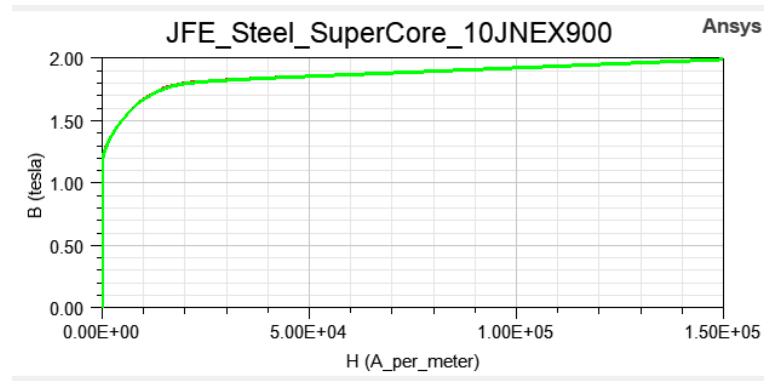
Today, the need to increase the efficiency of electrical machines and the magnetic materials used in the core structures provide less specific power losses thanks to thinner and higher magnetic flux density materials. The biggest problem in generator design in general is that the manufacturing process can be subjected to mechanical stress and thermal stress that can degrade the magnetic quality of the core materials. In addition, with the current knowledge, the rate of deterioration of the core materials during generator manufacturing is not linear and cannot be predicted exactly. Therefore, the magnetic measurement techniques must be developed and applied to assess the quality of core materials at various stages of the manufacturing [27, 28].



(a)



(b)



(c)

**Figure 2.** B–H curve comparison of the core materials, (a) M19\_24G, (b) 2605SA1 core, (c) 10JNEX900 core.

In order to obtain the properties of magnetic materials used in the stator and rotor core parts of electric motors and generators in general, core material manufacturers present them as datasheets after experimental studies according to IEC 60404-6. B-H curves are magnetization curves describing the saturation flux and magnetic field strength values of the materials. In addition, specific power loss values for flux values up to saturation point according to operating frequency values are given with graphics.

The technical specs of the core materials are given in the material library of the FEA software, and if a different material is to be used, the B-H values and the B-P values showing the specific power losses can be added to the material library of the software. B–H curves of three different core materials used in this study are given in comparison with Figure 2 (a), (b), and (c), respectively [29]. As the supply frequency increases in asynchronous motors, the losses in the magnetic core increase and gradually begin to dominate. Therefore, lamination of reduced specific power losses, especially amorphous steel and JFE supercore, is recommended to increase efficiency in such machines. However, such laminations tend to have lower repellent magnetizing properties, which may affect the running characteristics of the motor, and are referred to as soft core material [30].

**Table 1.** Comparison the technical specs of the core materials [31,32,33,34,35,36]

Parameters	Core Material Type		
	Conventional	Amorphous	JFE
Material Content	FeSi(3%)	Fe(80%)Si(9%)B(11%)	FeSi(6.5%)
Saturation Flux Density [T]	1.7	1.56	1.9
Relative Permeability, [ $\mu_r$ ]	4000	20000	23000
Curie Temperature [ $^{\circ}$ C]	550	395	700
Coercivity Force, $H_c$ [A/m]	150	4	30
Mass Density [kg/m <sup>3</sup> ]	7650	7330	7490
Thickness of material [mm]	0.35	0.025	0.10
Stacking Factor	0.98	0.83	0.95
Electrical Resistivity [ $\mu\Omega$ m]	0.82	1.37	0.72
Hysteresis loss coefficient (Kh)	172.842	22.292	133.474
Eddy-current loss coefficient (Ke)	1.3684	1.173	0.01346
Specific Core Loss (W/kg at 50 Hz)	3.3	0.14	1.17
Thermal Conductivity [(W/m K)]	53	10	19.6
Manufacturer and Material Code	Cogent M19-24G (M330-350A)	Metglas 2605SA1	JFE Steel 10JNEX900

The core material, which is frequently used in the design of stator and rotor parts of electric motors in general, is a 0.35 mm thickness of 3% SiFe alloy, also known as M19\_24G type motor sheet. The specific core loss value of this core material is 3.3 W/kg for an operating frequency of 50 Hz and a flux density of 1.5 T. In addition, the JFE supercore core material, which has become popular in recent years, is commercially available with a lamination structure three times thinner than the M19\_24G core material. The saturation flux density value of this material is 1.9 T and the specific core loss value is 1.7 W/kg, which remains quite low. In addition, the permeability of 10JNEX900 core material as JFE supercore as 6.5% SiFe for 0.10 mm thickness is approximately five times that of conventional core material for 0.10 mm thickness. Ribbon steel, with a thickness of 0.025 mm as amorphous core material, is often used in inductor and transformer design with much lower magnetic field strength values and much lower specific core loss values as soft magnetic material [31]. Comparative specs of core materials with these three different characteristics are given in Table 1. [32, 33, 34, 35, 36].

## 2.2. FEA modelling methodology

In order to design and simulate electrical machines (such as transformers, electric motors and generators, etc.) with ANSYS-Maxwell software, the steps followed in electromagnetic modeling are followed systematically as given in Figure 3. After determining the solution type in the steps given in the flow diagram, 2D/3D geometric drawings of electrical machines, meshing operations and excitation conditions should be assigned for electromagnetic modeling. In the analysis settings stage, simulation conditions are determined for the solution setup. According to the technical data obtained from FEA simulation studies, reports such as numerical values such as current, voltage, inductance and power losses, 2D/3D graphics and flux distributions are received [37, 38].

The power electronics circuits and FEA modeling equivalent circuits are run by co-simulation, and both power electronics circuit performance and synchronous generator performance can be considered together. Thus, the performances of electrical machines and power electronic circuits can be tested in detail before experimental studies are carried out. Electromagnetic modeling analysis using FEA consists of three stages: preprocessing, field solution, and postprocessing. In the preprocessing stage, the geometry is developed, the problem is defined (core material selection, the nonlinear characteristics of ferromagnetic iron are introduced, magnetization of the magnets in the required direction) and the mesh is produced. Electromagnetic modelling is performed using FEA software, which is a powerful tool for the design of electrical machines and other electrical systems [23].

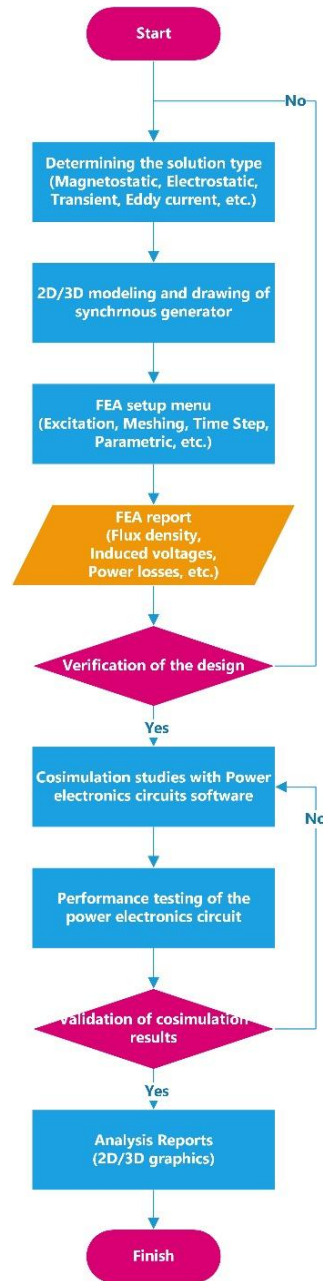


**Figure 3.** FEA modelling methodology flowchart

### 2.3. Theoretical background for CPSGs

Generally, the synchronous generator induction principle and theory apply. Thus, the phase EMF in the stator windings of a claw-pole synchronous generator whose stator windings are designed with 120 electrical degrees of phase difference can be given as Equation 1 [23]:

$$e_f = \Phi N_w k_b n_r \quad (1)$$

where,  $\Phi$  represents the magnetic flux,  $N_w$  is the number of turns for stator winding,  $k_b$  is the winding factor, and  $n_r$  is the rotor speed as rpm.

The calculation of the magnetic flux induced by one full rotation of the permanent magnet rotor in the stator depends on the magnetic field intensity. In addition, the rotor structure of the claw pole alternator is different from ordinary generators and has a cylindrical pole structure surrounded by claw-shaped soft iron parts. The modeled CPSG has a full mold three-phase winding structure and a cylindrical claw structure rotor with 4-pole placed on the 24-slot stator. In steady state, the expression for the current of the stator windings with the dq0 conversion is given by Equation 2 [22]:

$$\begin{bmatrix} I_d \\ I_q \\ I_o \end{bmatrix} = \frac{2}{3} \begin{bmatrix} \cos \varphi & \cos\left(\varphi - \frac{2\pi}{3}\right) & \cos\left(\varphi - \frac{4\pi}{3}\right) \\ -\sin \varphi & -\sin\left(\varphi - \frac{2\pi}{3}\right) & -\sin\left(\varphi - \frac{4\pi}{3}\right) \\ \frac{1}{2} & \frac{1}{2} & \frac{1}{2} \end{bmatrix} \begin{bmatrix} I_a \\ I_b \\ I_c \end{bmatrix} \quad (2)$$

Thus, the three-phase stator currents that are 120 degrees electrically out of phase between them can be clearly written as  $I_a$ ,  $I_b$ , and  $I_c$ , respectively, with Equations 3-5:

$$I_a = I_p \cos(\omega t + \varphi) \quad (3)$$

$$I_b = I_p \cos\left(\omega t + \varphi - \frac{2\pi}{3}\right) \quad (4)$$

$$I_c = I_p \cos\left(\omega t + \varphi - \frac{4\pi}{3}\right) \quad (5)$$

where,  $I_p$  is the peak value of the stator phase current. Stator phase voltages for d-q axis are given in Equations 6-7:

$$V_d = I_d r_a + \frac{d\psi_d}{dt} - \omega \psi_q \quad (6)$$

$$V_q = I_q r_a + \frac{d\psi_q}{dt} - \omega \psi_d \quad (7)$$

The stator winding fluxes can be expressed by Equations 8-9 for the d-q axis form:

$$\psi_d = -I_d L_d + I_f L_{afd} \quad (8)$$

$$\psi_q = -I_q L_q \quad (9)$$

Thus, the direct-axis reactance and quadrature-axis reactance of CPSG can be expressed as Equations 10-11 in the form of the d-q axis:

$$X_d = \frac{\omega_b L_d}{Z_b} \quad (10)$$

$$X_q = \frac{\psi_q}{I_q} \quad (11)$$

Finally, the expression for the induced EMF per phase of a synchronous generator can be given by Equation 12:

$$E_{ph} = 4.44 K_{w1} \Phi_m f N_w \quad (12)$$

where,  $\Phi_m$  represents the maximum flux circulating between the stator and rotor cores, and  $f$  represents the frequency. Also,  $N_w$  is total number of turns per stator phase. Also, a simplified expression for the EMF value induced in the stator windings can be written as Equation 13 [7]:

$$E_{ph} = \frac{1}{\sqrt{2}} N_w \omega \Phi_m \quad (13)$$

The cogging torque ( $T_{cog}$ ) of synchronous generators is a periodic torque oscillation without any excitation current which can be derived with Equation 14 [13]:

$$T_{cog} = \frac{1}{2} \Phi^2 \frac{d\mathfrak{R}}{d\theta} \quad (14)$$

where  $\theta$  is the rotor position angle,  $\Phi$  is the main flux, and  $\mathfrak{R}$  is the general magnetic circuit reluctance of the CPSG core.

#### 2.4. Efficiency and Power Losses

In general, eddy current loss ( $P_{edd}$ ) accounts for most core losses, depending on the lamination thickness of the core material. Hysteresis losses ( $P_{hys}$ ) occur with the change of direction of the magnetic field poles depending on the frequency. However, in case of poor heat dissipation of the core material, eddy current loss also causes higher temperature to rise in the core parts. The losses of the stator windings ( $P_{cu}$ ) depend on the square of the current and the resistance values ( $R_c$ ) of the windings, as given by Equation 15, and are released as heat. The core losses can be given with Equations 16-17 for CPSG, and Equation 18 is given for efficiency ( $\eta$ ) [10, 21].

$$P_{cu} = R_c I^2 \quad (15)$$

$$P_{hys} = K_h f B_m^{1.6} \quad (16)$$

$$P_{edd} = K_e f^2 B_m^2 \quad (17)$$

$$\eta = \frac{P}{P + P_{cu} + P_{hys} + P_{edd}} \quad (18)$$

where,  $P$  is the electrical power from the generator,  $B_m$  is the magnetic flux density, and  $K_h$  and  $K_e$  are the coefficients for the hysteresis and eddy current losses of the core material, respectively.

### 3. MODELLING of CPSG with FEA SOFTWARE

In general, CPSGs can be classified as synchronous generators. However, the operating conditions of HEVs are quite different from other generator applications. The armature current is very large due to the low battery voltage level connected to the alternator. The stator and rotor core parts are highly saturated due to machine size limitations. Therefore, it is very difficult to fully apply the design methodologies of other synchronous generators to CPSGs. For example, the technical characteristics of the alternator cannot be accurately predicted by magnetic equivalent circuits whose parameters are determined under linear superposition assumptions based on classical mathematical expressions using no-load voltage and armature reaction. Three-dimensional (3D) electromagnetic field analysis is generally applied in many papers in the past literature that propose modeling methodology with FEA software to predict the properties of CPSGs [5].

Finite Element analysis (FEA) 3D software can be used directly to accurately predict the electrical and mechanical behavior of machines. However, electromagnetic modeling the claw poles is difficult, as it requires a lot of computation time and memory, and using 3D FEA in the initial design is not recommended [39]. Therefore, CPSG was first performed with a short one-dimensional analysis using the ANSYS-Rmxprt module. In this context, winding structures and core materials can be assigned by sizing the stator and rotor parts of the generator.

ANSYS-Rmxprt academic version software is used primarily for the electromagnetic modeling of the three-phase CPSG, and the three-phase 24-slot stator shown in Figure 4(a) and the proposed example as a permanent magnet excited 4-pole rotor structure are selected. To compare the stator core structure, three different core materials, namely M19\_24G (3% SiFe), 2605SA1 (Amorphous) and 10JNEX900 (6.5% JFE supercore), are determined and sizing processes are carried out according to the specs given in Table 2. The full slot pitch for the stator phase windings is  $24/4=6$  according to the number of stator slots and the number of poles in the rotor, but in this modeling, the slot pitch is set as 2-7 as seen in Figure 4(b) with a step abbreviation.

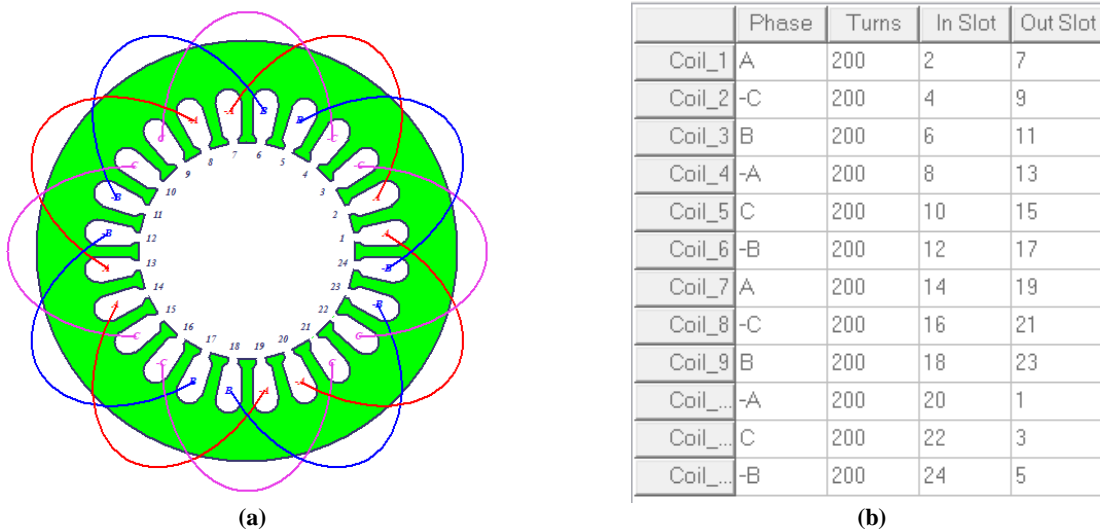


**Figure 4.** CPSG phase windings, (a) stator winding arrangement and (b) edited winding layout.

The stator phase windings consist 200 turns, and placed in the stator slots with 120 electrical degrees between them. Thus, the CPSG is designed as if it were fabricated in a virtual environment and can be simulated almost realistically.

**Table 2.** CPSG's modelling specs [40]

Parameters	Value
Rated apparent power	0.55 kVA
Rated power factor	0.71
Number of phases	3
Rated voltage	115 V
Frequency	50 Hz
Stator outer diameter	120 mm
Stator inner diameter	80 mm
Stator length	65 mm
Number of stator slots	24
Stator core material	*Comparative analysis
Stacking factor	0.95
Rotor outer diameter	78.8 mm
Rotor inner diameter	12 mm
Rotor length	80 mm
Rotor yoke diameter	50 mm
Rotor core material	Steel_1008
Number of rotor poles	4
Pole magnet type	XG196/96_3DSF1.000_X
Length of Magnet	10 mm
Air-gap length	0.60 mm
Rated synchronous speed	1500 rpm
Load type	Infinite bus

The cross-sectional view of the claw pole structure on the rotor is as in Figure 5 in the sizing section of ANSYS-Rmxprt. Therefore, many changes regarding dimensioning such as rotor and pole lengths, pole foot thickness and yoke diameter dimensions, slot depth, shaft diameter can be made as desired.

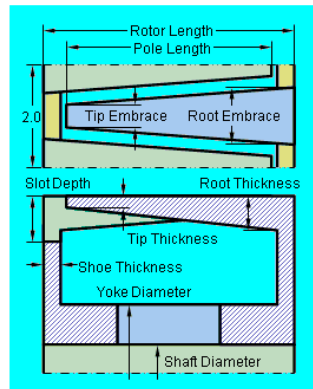


**Figure 5.** Sizing parameters of claw pole rotor [40].

The rotor and pole structure of the modeled CPSG is shown in Figure 6. An extremely powerful magnet is used with a disk-shaped XG196/96\_3DSF1.000\_X type Coercive Force value of 690 kA/m and Residual Flux Density 0.96 T, which provides the excitation of the rotor poles.

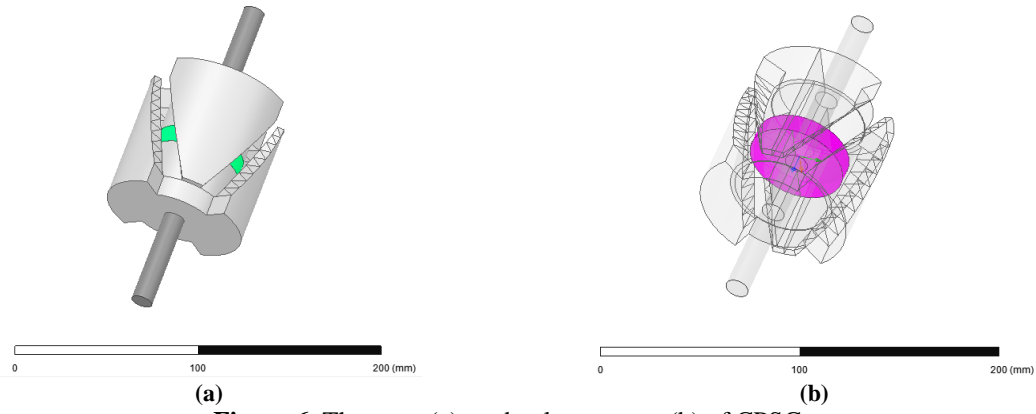


**Figure 6.** The rotor (a), and pole structure (b) of CPSG.

The claw pole structure of the rotor resembles a crankshaft and can produce voltage in sinusoidal wave form with its cylindrical pole structure. The full modeling image for the CPSG with the stator windings is given in Figure 7. The stator windings are essentially like the stator windings of a three-phase asynchronous motor and are placed with a 120-degree electrical angle between them.

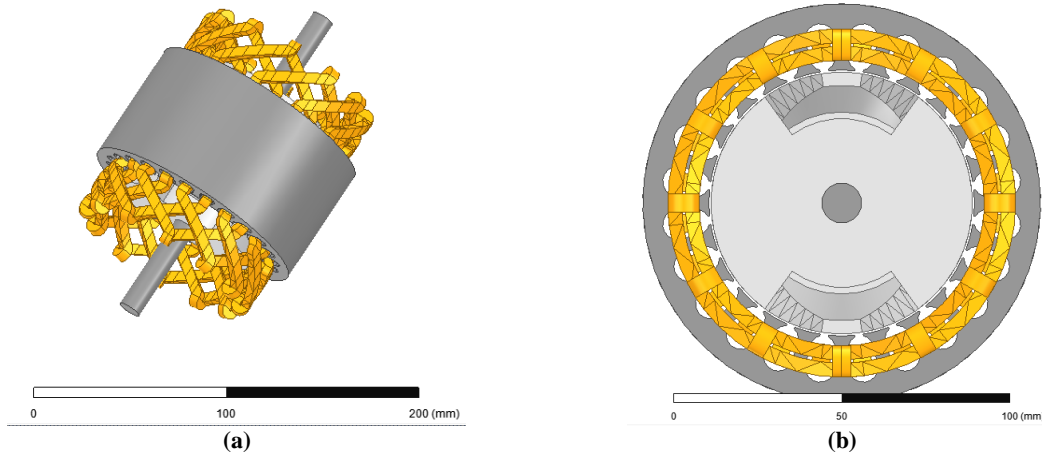


**Figure 7.** The full modeling 3D image for the CPSG, (a) 3D image, (b) front view of generator.

The meshing process for CPSG modeled in 3D with Maxwell software is given in Figure 8. Mesh refinement is very important for the convergence of the solution results, but at this point, the performance of the computer running the software comes to the fore. In fact, the better the RAM memory capacity in performing the meshing process, the more the solution start time changes. Since Maxwell software solves according to the finite element method, if the meshing process fails, it cannot proceed to the solution. The solution process depends on the processor capacity and memory capacity of the computer. The technical features of the computer used in this study can be summarized as i7-8 cores, 16 GB RAM and 250 GB SSD. As the meshing precision increases, the running times of the software also change.

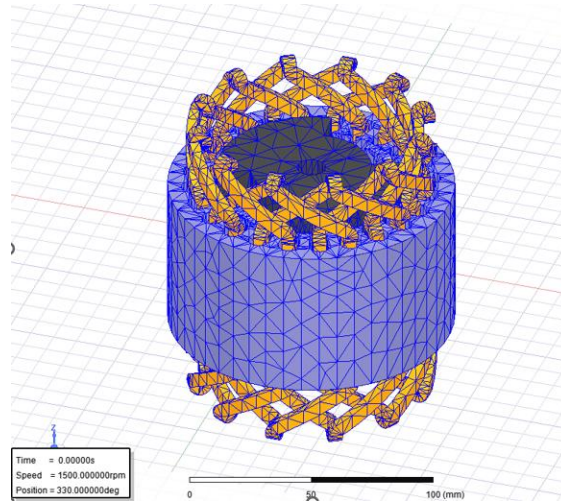


**Figure 8.** Mesh refinement of CPSG.

The power losses and efficiency of the CPSG, whose electromagnetic modeling was performed with ANSYS-Electronics Rmxprt and Maxwell software, according to the full load technical data information, are explained in detail in Table 3.

**Table 3.** Full load technical data of the modeled CPSG.

Parameters	Value
Stator Phase Current (rms)	1.6 A
Stator Phase Voltage (rms)	115 V
Apparent Power	0.55 kVA
Power Factor (Cos $\phi$ )	0.98
Induced Phase Voltage (rms)	152.7 V
Frictional and Windage Losses	24 W
Core Losses	4.25 W for M19_24G core material
Stator Copper Losses	72.45 W
Total Losses	100.7 W
Output Electrical Power	539.897 W
Input Mechanical Power	640.597 W
Efficiency (%)	84.28%
Maximum Output Power	669.41 W

Even when only core losses are considered, CPSG performance varies significantly with core material type. According to the graph given in Figure 9, the core loss behavior of the generator designed with Amorphous, 3%SiFe and JFE super core material is given comparatively.

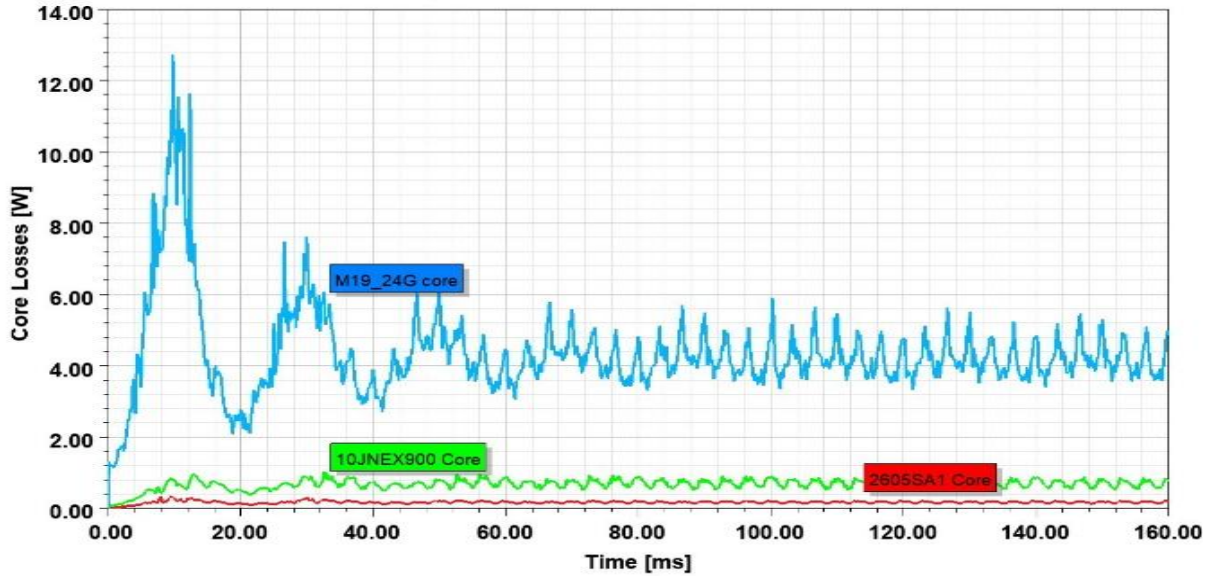


**Figure 9.** The core loss behavior of CPSG designed with M19\_24G, Amorphous and JFE super core materials.

Thus, it was determined that the most suitable core material in terms of core losses was 2605SA1 core. M19 core, known as the classical core lamination, used in the application, is the worst material in terms of core losses and the core material where the temperature increase will be the highest. In addition, winding losses for CPSG are also examined comparatively. In fact, winding losses are the most important cause of thermal increase in a generator, and a slight difference was observed in winding losses due to reasons such as inductance that changes according to the core material type. Thus, according to the comparative winding losses graph given in Figure 10, the most loss emerges as the classical core material M19. The winding loss behavior for the other two materials (Amorphous and JFE super core) is almost the same.

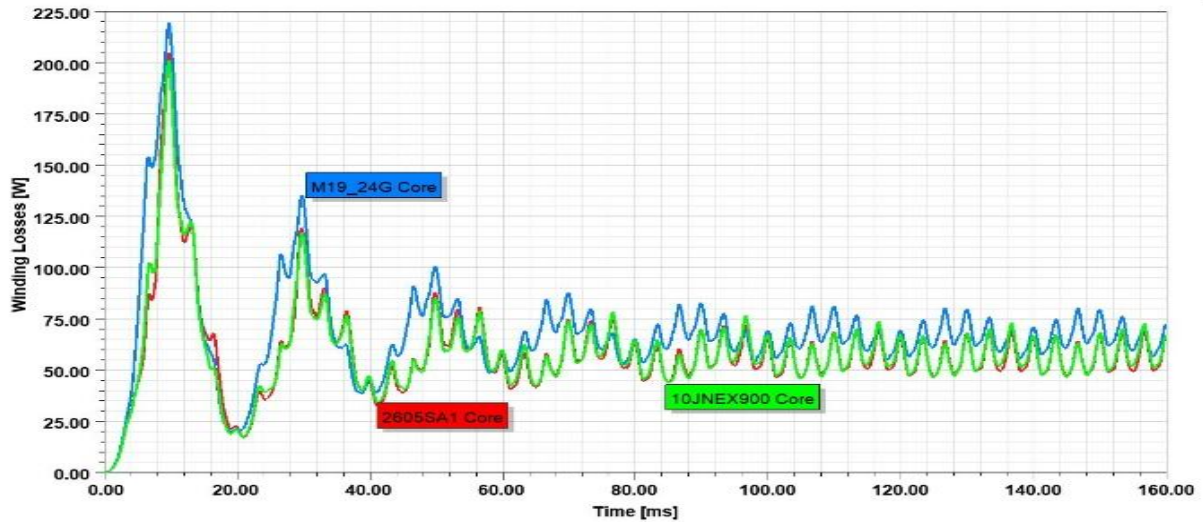


**Figure 10.** The copper loss behavior of CPSG designed with M19\_24G, Amorphous and JFE super core materials.

Thus, it is summarized in Table 4 that higher efficiency can be obtained with the new generation core materials for CPSG, which is analyzed comparatively according to the core material type.

**Table 4.** The power losses and efficiency comparison of CPSG according to core material type

Comparison of Parameters	Core Material Type		
	M19_24G	10JNEX900	2605SA1
Frictional and Windage Losses	24 W (fixed)	24 W (fixed)	24 W (fixed)
Core Losses	4.25 W	0.75 W	0.35 W
Stator Copper Losses	72.45 W	55.82 W	55.35 W
Total Losses	100.70 W	80.57 W	79.70 W
Efficiency (%)	84.28%	87.02%	87.13%

The highest efficiency is achieved with amorphous material, but the design is limited to this material according to the structural features of the stator grooves. Because amorphous materials are very hard and not resistant to mechanical stresses with their crystallized film feature. However, JFE supercore material has almost the same efficiency as amorphous. The core material type is also extremely important in terms of torque behavior as seen in Figure 11. The core material with the least torque fluctuation can be summarized as a JFE core with a high flux density of 1.9 T and a non-oriented core material.

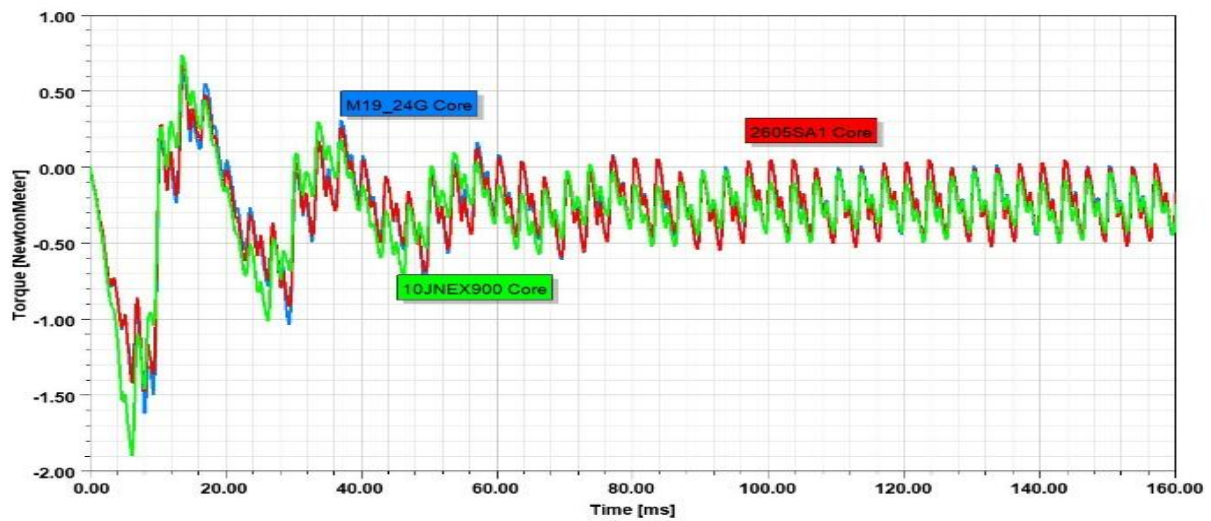


**Figure 11.** The torque behavior of CPSG designed with M19\_24G, Amorphous and JFE super core materials.

The flux distributions in the CPSG core for the different core materials are given in Figure 12 in 2D. Since the saturation flux value for M19 is 1.7 Tesla, it is seen that it is very close to the saturation point. There is no saturation for the JFE supercore, which has a saturation flux value of about 1.9 T. For amorphous with a saturation flux value of 1.56 T, there are regions close to the saturation point. However, since it is a soft magnetic material due to its amorphous structure, the canceling magnetic field strength is very small, and the thermal coefficient and specific core loss are at the lowest values.

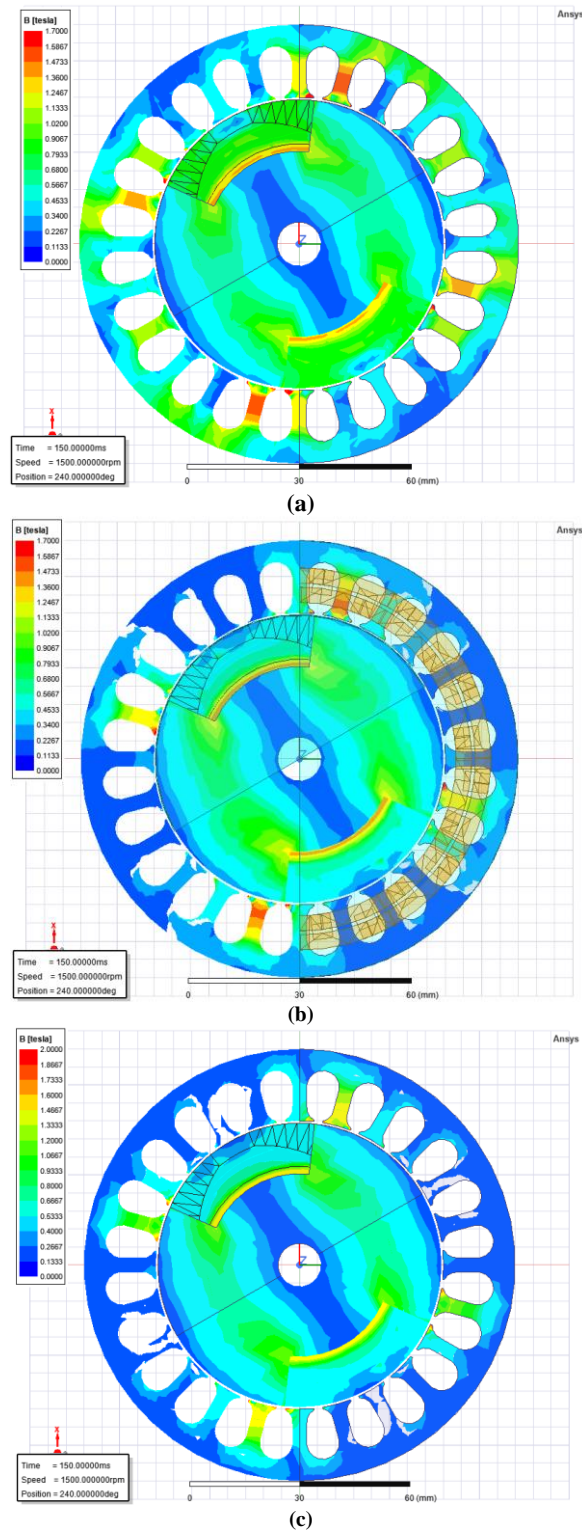


**Figure 12.** The flux distributions of CPSG core, (a) M19\_24G core, (b) amorphous core, (c) JFE supercore.

The findings obtained because of the modeling and simulation studies of the CPSG performed with the FEA software can be listed as follows, comparatively according to the core material type:

- M19 classical core material is widely used in practice.

- When the core loss behavior is examined, M19 core material is the most unsuitable material.

•JFE supercore core loss is higher than amorphous material core loss values, but when design and manufacturing are considered, amorphous material is not very suitable for the design of stator slots. Amorphous material is mostly recommended for inductor and transformer design.

- JFE supercore is the most suitable material in terms of electromagnetic and torque performance.

•In recent years, JFE supercore material has become popular both in electric motor design [33] and generator design in terms of power losses and temperature behavior compared to M19 material. It also allows more compact design such as core size reduction in motor/generator sizing.

•Although the classical core material (M19) is much cheaper than the new generation core materials, the new generation core materials can be preferred for high efficiency CPSG designs due to their more compact design and lower power loss values.

•The core material comparison discussed in this study highlights that JFE supercore material is very suitable for performance enhancement for CPSG, which is frequently used in ICE and hybrid electric vehicles in recent years.

•It is known that if the magnetic properties of the core materials are taken into account in the design process of the CPSG dimensioning, it may lead to structures with different sizes. However, in this study, a short performance comparison was performed using different magnetic materials for 0.55 kVA power. Thus, it was seen that even for the same size, the power loss values of the new generation core materials were lower, and the performance was improved.

•Maybe a few W core and winding losses will be reduced, but CPSGs, which are used as battery charging units for millions of vehicles, can be used in the coming years for much larger power capacities, especially in the stator core structures of wind generators. In this context, JFE supercore material is advantageous in terms of high flux density, much finer lamination, and much smaller specific core losses.

#### 4. CONCLUSION

In this study, the electromagnetic modeling and simulation studies of performance improvement are carried out by using new generation core materials of CPSG, which is frequently used as a battery charging alternator of ICE vehicle. Since the new generation core materials are produced with higher magnetic flux density and much thinner structures than conventional core laminations, they have become the focus of attention in recent years with less specific core loss values. In particular, the need for a more compact design and higher efficiency in the power system for energy storage in hybrid electric vehicles has also intensified the efforts to increase the performance of CPSGs.

The CPSG considered in this study is only 0.55 kVA power value, and this will gain more importance as the power values increase, as the lamination material used in the core structure will increase. On the other hand, when it is used in internal combustion land vehicles and considering millions of places of use, a reduction in power loss of a few W may positively affect many factors such as the global economy and environmental pollution. M19\_24G core material is commercially easily available compared to others, but considering its performance characteristics such as size, power losses and temperature behavior, it will leave its place to new generation core materials as the technology of the future. Depending on the core material type, the CPSG efficiency was determined as 84.28% for the classical core material M19, 87.02% for the jfe supercore, and 87.13% for the amorphous core material, respectively. Thus, it is seen that the CPSG designed with the new generation core materials has higher efficiency. As a future study, a CPSG can be designed using new generation core materials, for example, with jfe supercore, and its sizing, electrical and electromagnetic behavior can be determined experimentally.

## REFERENCES

1. Nasiri-Zarandi, R., Mohammadi Ajamloo, A., and Abbaszadeh, K. Cogging Torque Minimization in Transverse Flux Permanent Magnet Generators using Two-step Axial Permanent Magnet Segmentation for Direct Drive Wind Turbine Application. *International Journal of Engineering*, 34(4), 2021, 908-918. doi: 10.5829/ije.2021.34.04a.17.
2. Jurca, F., Martis, C., and Biro, K. Claw-pole generator analysis using flux 3D, *International Symposium on Power Electronics, Electrical Drives, Automation and Motion*, Ischia, Italy, 2008, pp. 1286-1291, doi: 10.1109/SPEEDHAM.2008.4581153.
3. Boldea, I., Tutelea, L. N., and Popa, A. A. "Claw Pole Synchronous Motors/Generators (CP-SMs/Gs) Design and Control: Recent Progress," in *IEEE Journal of Emerging and Selected Topics in Power Electronics*, vol. 10, no. 4, pp. 4556-4564, Aug. 2022, doi: 10.1109/JESTPE.2021.3125044.
4. Wang, X., Yuan, P., Li, Y., Chen, S., Shi Z., and Xie W., Performance research and optimization of vehicle-mounted claw-pole generator based on 3D electromagnetic field and circuit coupling modeling, *IEEE International Power Electronics and Application Conference and Exposition (PEAC)*, Guangzhou,Guangdong, China, 2022, pp. 886-891, doi: 10.1109/PEAC56338.2022.9959606.
5. Yamazaki, K., Suzuki, R., Nuka, M., and Masegi, M. Analysis and Characteristics Improvement of Claw-Pole Alternators by Reducing Armature Reaction, in *IEEE Transactions on Industrial Electronics*, vol. 65, no. 11, pp. 8740-8748, Nov. 2018, doi: 10.1109/TIE.2018.2811405.
6. Ibala, A. and Masmoudi, A. 3D-FEA based comparison of the features of two hybrid-excited claw pole alternators, *International Conference on Sustainable Mobility Applications, Renewables and Technology (SMART)*, Kuwait, Kuwait, 2015, pp. 1-8, doi: 10.1109/SMART.2015.7399239.
7. Cao, Y., Liu, C., and Yu, J. Mesh-Based 3D MEC Modeling of a Novel Hybrid Claw Pole Generator. *Energies* 2022, 15, 1692. <https://doi.org/10.3390/en15051692>.
8. Kuroda, Y., Morita, M., Hazeyama, M., Azuma, M., and Inoue, M. Improvement of a claw pole motor using additional ferrite magnets for hybrid electric vehicles, *The XIX International Conference on Electrical Machines - ICEM 2010*, Rome, Italy, 2010, pp. 1-3, doi: 10.1109/ICELMACH.2010.5608267.
9. Emadi, A., Lee, Y. J., and Rajashekara, K. Power electronics and motor drives in electric, hybrid electric, and plug-in hybrid electric vehicles, *IEEE Trans. Ind. Electron.*, vol. 55, no. 6, pp. 2237-2245, Jun. 2008.
10. Du, W., Zhao, S., Zhang, H., Zhang, M., and Gao, J. A Novel Claw Pole Motor With Soft Magnetic Composites, in *IEEE Transactions on Magnetics*, vol. 57, no. 2, pp. 1-4, Feb. 2021, Art no. 8200904, doi: 10.1109/TMAG.2020.3019830.
11. Bruyere, A., Semail, E., Bouscayrol, A., Locment, F., Dubus, J. M., and Mipo, J. C. Modeling and control of a seven-phase claw-pole integrated starter alternator for micro-hybrid automotive applications, *IEEE Vehicle Power and Propulsion Conference*, Harbin, China, 2008, pp. 1-6, doi: 10.1109/VPPC.2008.4677668.
12. Suh, K. and Moon, J. Electric Vehicle Architecture Design Based on Database. *Int.J Automot. Technol.* 25, 2024, 427-444, <https://doi.org/10.1007/s12239-024-00035-5>.
13. Zhao, X., Niu, S., and Ching, T. W. Design and Analysis of a New Brushless Electrically Excited Claw-Pole Generator for Hybrid Electric Vehicle, in *IEEE Transactions on Magnetics*, vol. 54, no. 11, pp. 1-5, Nov. 2018, Art no. 8108505, doi: 10.1109/TMAG.2018.2823743.
14. Ming-Fa Tsai et al. Phase-Variable Modeling and Comparative Study between a PMA-CPA and a CPA Alternator by Simulation Analysis 2022 *J. Phys.: Conf. Ser.* 2179 012014.
15. Toprak, Y., Karakaya, O., Canturk, S., and Balci, M.E., Analysis on Performance of Claw Pole Synchronous Generators for 6-Pulse Rectifier Load, *4th International Turkish World Engineering and Science Congress*, 2023, Türkiye.
16. Toprak, Y., Karakaya, O., Canturk, S., and Balci, M.E., Design of Passive Harmonic Filter for the Claw-Pole Synchronous Generators under Non-linear Loading, *The 3rd International Conference on Applied Mathematics in Engineering (ICAME'24)*, 26-28 June 2024, Ayvalık, Balıkesir, Türkiye.
17. Saati, M., Hashemipour, O., Afjei, E., and Nezamabadi, M. A New Hybrid Brushless DC Motor/Generator without Permanent Magnet. *International Journal of Engineering*, 20(1), 77-86, 2007.
18. Cao, Y., Zhu, S., Yu, J., and Liu, C. Optimization Design and Performance Evaluation of a Hybrid Excitation Claw Pole Machine. *Processes* 2022, 10, 541. <https://doi.org/10.3390/pr1003054>.
19. Li, W. and Huang, S. Analysis and Design of Hybrid Excitation Claw-pole Generator, *Electric Power Components and Systems*, 39:7, 680-695, 2011, DOI: 10.1080/15325008.2010.536811.
20. Zhang, D., Zhao, C., Zhu, L., Ding, Y., Yu, C., and Tian, C. On hybrid excitation claw-pole synchronous generator with magnetic circuit series connection, *International Conference on Electrical Machines and Systems*, Wuhan, China, 2008, pp. 3509-3513.

21. Ukaji, H., Hirata, K., and Niguchi, N. Claw pole magnetic-gear generator for hub dynamos, International Conference on Electrical Machines (ICEM), Berlin, Germany, 2014, pp. 416-421, doi: 10.1109/ICELMACH.2014.6960214.
22. Arumugam, D., Logamani, P., and Karuppiyah, S. Improved performance of integrated generator systems with claw pole alternator for aircraft applications, Energy, Volume 133, 2017, Pages 808-821, <https://doi.org/10.1016/j.energy.2017.05.132>.
23. Liang, J., Parsapour, A., Cosoroaba, E., Wu, M., Boldea, I., and Fahimi, B. A High Torque Density Outer Rotor Claw Pole Stator Permanent Magnet Synchronous Motor, IEEE Transportation Electrification Conference and Expo (ITEC), Long Beach, CA, USA, 2018, pp. 389-393, doi: 10.1109/ITEC.2018.8450106.
24. Shen, J., Wang, B., Cai, L. et al. Magnetic properties and thermal stability of Fe-based amorphous/carbonyl iron soft magnetic composites. J Mater Sci: Mater Electron 34, 1169, 2023, <https://doi.org/10.1007/s10854-023-10512-9>.
25. Guo, Y., Zhu, J., and Dorrell, D. G. Design and Analysis of a Claw Pole Permanent Magnet Motor with Molded Soft Magnetic Composite Core, in IEEE Transactions on Magnetics, vol. 45, no. 10, pp. 4582-4585, Oct. 2009, doi: 10.1109/TMAG.2009.2022745.
26. Rakotovoao, M. Modeling approach for system analysis: Case of claw pole machine in mild hybrid system, XXII International Conference on Electrical Machines (ICEM), Lausanne, Switzerland, 2016, pp. 818-822, doi: 10.1109/ICELMACH.2016.7732620.
27. Clerc, A. J. and Muetze, A. Measurement of stator core magnetic characteristics, IEEE International Electric Machines & Drives Conference (IEMDC), Niagara Falls, ON, Canada, 2011, pp. 1433-1438, doi: 10.1109/IEMDC.2011.5994818.
28. Khan, M. A., Chen, Y., and Pillay, P. Application of soft magnetic composites to PM wind generator design, IEEE Power Engineering Society General Meeting, Montreal, QC, Canada, 2006, pp. 4 pp.-, doi: 10.1109/PES.2006.1709048.
29. Tong, W., Sun, R., Zhang, C., Wu, S., and Tang, R. Loss and Thermal Analysis of a High-Speed Surface-Mounted PMSM With Amorphous Metal Stator Core and Titanium Alloy Rotor Sleeve, in IEEE Transactions on Magnetics, vol. 55, no. 6, pp. 1-4, June 2019, Art no. 8102104, doi: 10.1109/TMAG.2019.2897141.
30. Dems M. and Komez, K. Performance Characteristics of a High-Speed Energy-Saving Induction Motor with an Amorphous Stator Core, in IEEE Transactions on Industrial Electronics, vol. 61, no. 6, pp. 3046-3055, June 2014, doi: 10.1109/TIE.2013.2251739.
31. Hasegawa, R. Applications of amorphous magnetic alloys, Materials Science and Engineering: A, Volumes 375-377, 2004, Pages 90-97, <https://doi.org/10.1016/j.msea.2003.10.258>.
32. Battal, F., Balci, S., and Sefa, I. Power electronic transformers: A review, Measurement, Volume 171, 2021, 108848, <https://doi.org/10.1016/j.measurement.2020.108848>.
33. Balci, S. and Akkaya, M. Reduction of the core size and power losses by using soft magnetic material for a single-phase induction motor, Measurement, Volume 198, 2022, 111421, <https://doi.org/10.1016/j.measurement.2022.111421>.
34. M19\_24G Core Material Datasheet, Non-Oriented Fully Process Electrical Steel – ASTM, <https://www.scribd.com/document/98899985/Non-Oriented-Fully-Process-Electrical-Steel-ASTM>.
35. Metglas 2605 SA1 Datasheet, Iron Based Alloy, <https://metglas.com/magnetic-materials/metglas-2605-sa1-iron-based-alloy-2/>.
36. 10JNEX900 Datasheet, Non-Oriented Electrical Steel Sheet, <https://www.jfe-steel.co.jp/en/products/electrical/product/supercore/index.php>.
37. Balci, S. Senkron Generatörlerde Farklı Stator Oluk Yapılarının Uç Gerilimine Etkisinin Sonlu Elemanlar Yöntemi ile Analizi, Bitlis Eren Üniversitesi Fen Bilimleri Dergisi, 8(3), 947-957, 2019, DOI: <https://doi.org/10.17798/bitlisfen.518348>.
38. Cheshmehbeigi, H. M. and Khanmohamadian, A. Design and Simulation of a Moving-magnet-type Linear Synchronous Motor for Electromagnetic Launch System, International Journal of Engineering (IJE), Transactions C: Aspects Vol. 30, No. 3, (March 2017) 351-356.
39. Soon-O. K., Ji-Young, L., Jung-Pyo, H., Yang-Soo, L., and Yoon, H. Practical analysis method for claw-pole type generator using 2-dimensional equivalent model, IEEE International Conference on Electric Machines and Drives, 2005., San Antonio, TX, USA, 2005, pp. 1661-1664, doi: 10.1109/IEMDC.2005.195942.
40. ANSYS Electronics 2024R1, Rmxprt User's Guide, Generators-CPSGs, 2024.